CORROSION SCIENCE AND TECHNOLOGY, Vol.2, No.4(2003), pp.189~193

A Study on the Plasma Etching of Ru Electrodes using O_2/Cl_2 Helicon Discharges

Hyoun Woo Kim and Woon Suk Hwang

School of Materials Science and Engineering, Inha University
253 Yong Hyeon Dong, Nam Gu, Incheon 402-751, Korea

The Ru etching using O_2/Cl_2 plasmas has been studied by employing the helicon etcher. The changes of Ru etch rate, Ru to SiO_2 etch selectivity and Ru electrode etching slope with varied process variables were investigated. The Ru etching slope at the optimized etching condition was measured to be 84°. We reveal that the Ru etching using O_2/Cl_2 plasma generates the RuO_2 thin film. Possible mechanism of Ru etching is discussed.

Keywords : *Ru, etching, helicon, plasma.*

1. Introduction

As dimensions of dynamic random access memory (DRAM) devices are getting smaller, high dielectric materials such as barium strontium titanate (BST) and tantallium pentoxide (Ta_2O_5), need to be used for the fabrication of capacitor structure.[1),2)]

Although platinum (Pt) has commonly been utilized as an electrode material, Pt has a difficulty in patterning and thus in forming a bottom electrode. Several research groups have reported that obtaining a sufficient etch selectivity of Pt to the mask material is extremely difficult.[3)-6)]

On the other hand, ruthenium (Ru) is expected to be patterned by chemical etching because the volatile etch product can be produced during the etching process.[7),8)] Previous researchers reported that volatile RuO_4 can be generated from the RuO_2 which is an intermediate phase of the Ru etching reaction.

However, there are not many systematic studies on the basic characteristics of Ru etching. In this study, we report the etching characteristics of Ru using O_2/Cl_2 helicon plasma. We investigate the Ru etch rate, the Ru to SiO_2 mask etch selectivity, and the Ru etching slope with varied process conditions including $Cl_2/(O_2+Cl_2)$ gas flow ratio and bias power. We investigate the Ru surface after etching by employing Auger electron spectroscopy (AES), x-ray photoelectron spectroscopy (XPS), and transmission electron microscopy (TEM).

2. Experimental

A storage node pattern with a critical dimension (CD) of 0.15 μm was used in our experiments. Top view of the storage node pattern indicates that the storage node is an oval type and space CDs along the short axis and the long axis are 150 nm and 250 nm, respectively. The sample structure was substrate/ TiN 500 Å/ Ru 4000 Å/ TiN layer 600 Å/ SiO_2 mask 3000 Å. The SiO_2 mask, instead of photoresist mask, was used for patterning Ru, because oxygen gas was the main etchant in our experiments. The SiO_2 mask was patterned by $CF_4/N_2/Ar$ gas. The TiN layer was inserted between Ru and SiO_2 mask layer to prevent the contamination of etching chamber during SiO_2 mask etching due to Ru exposure. The TiN layer was patterned by Ar/Cl_2 gas. Since Ru cannot be etched by halogen gases only due to high boiling point of their etch products, we used O_2 and Cl_2 gases, expecting that the volatile RuO_4 is produced.[7),8)]

For Ru etching experiments, m=0 helicon etcher commercially available from Trikon, Inc. has been used. Helicon wave plasma sources were operated at the excitation frequencies of 13.56 MHz. During etching, the $Cl_2/(O_2+Cl_2)$ gas flow ratio was 0.1-0.3, the source power was 1000-2000 W, the bias power was 150-300 W, the magnetic field was 100-200 gauss, the pressure was 10-30 mTorr and the total gas flow rate was 50-300 sccm.

A scanning electron microscope (SEM) was used to measure the Ru etching slope and the Ru to SiO_2 etch selectivity. Ru surface after etching was analyzed by AES, XPS, and TEM.

3. Results and discussion

Fig. 1 shows the change of Ru etch rate, Ru to SiO_2 mask etch selectivity and etching slope with varying $Cl_2/(O_2+Cl_2)$ gas flow ratio ranging from 0.1 to 0.3, using O_2/Cl_2 helicon plasma. The source power, bias power, total gas flow rate and pressure are set to 2000 W, 150 W, 50 sccm and 30 mTorr, respectively. We reveal that the maximum etch rate of about 257 Å/min, Ru to SiO_2 mask etch selectivity of about 15.1, and the maximum etching slope of 81° are attained at the $Cl_2/(O_2+Cl_2)$ gas flow ratio of 0.2.

Fig. 2 shows the change of Ru etch rate, Ru to SiO_2 mask etch selectivity, and etching slope with varying bias power ranging from 150 to 300 W. The source power, total gas flow rate and pressure are set to 2000 W, 50 sccm and 30 mTorr, respectively. The $Cl_2/(O_2+Cl_2)$ gas flow ratio is set to 0.2.

Both the Ru etch rate and Ru etching slope increases with increasing bias power in the range of low bias power. However, the Ru to SiO_2 mask etch selectivity decreases with increasing bias power due to the significant increase of SiO_2 mask etch rate. We assume that etching of SiO_2 mask with O_2/Cl_2 gas proceeds mostly by ion bombardment, because increasing the bias power helps to increase the ion bombardment energy. Since the increase of SiO_2 mask etch rate with increasing bias power is more significant than the increase of Ru etch rate, we surmise that chemical etching and thus radicals plays a role in Ru etching.

In order to investigate the effect of Ar addition, we have used O_2/Cl_2 helicon plasma with a total flow rate of 50

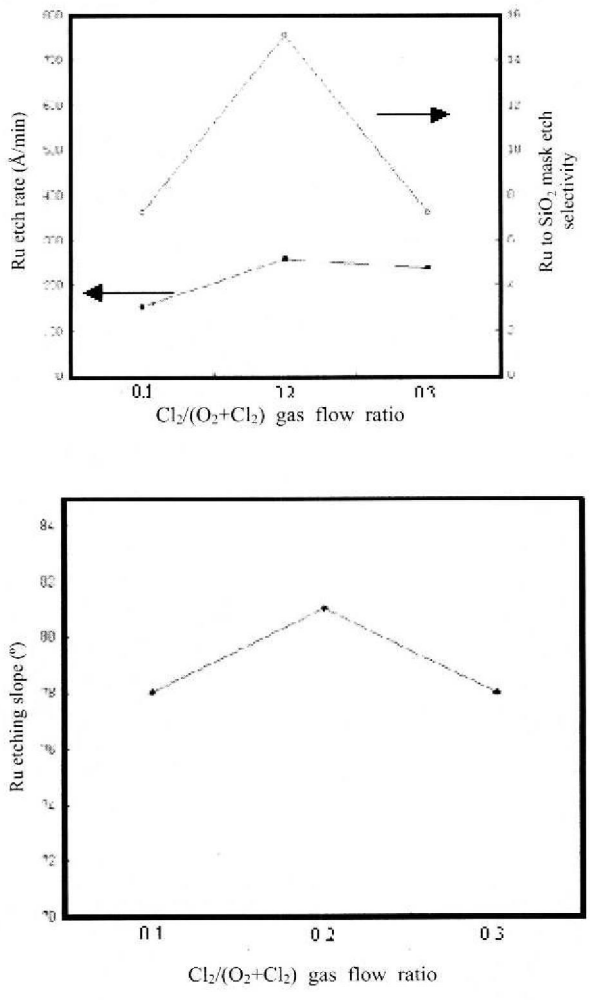

Fig. 1. Variation of Ru etch rate, Ru to SiO_2 mask etch selectivity and etching slope with varying $Cl_2/(O_2+Cl_2)$ gas flow ratio.

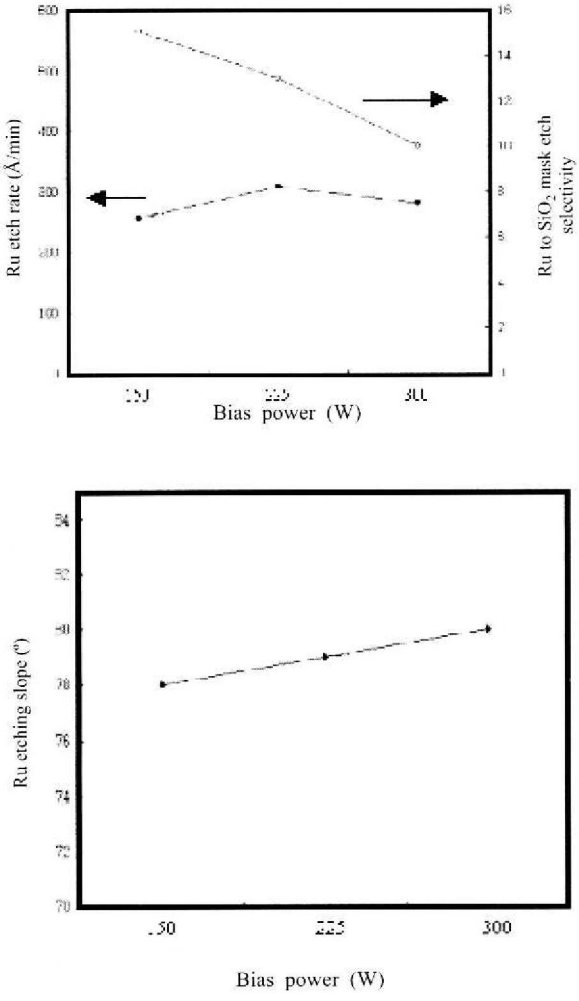

Fig. 2. Variation of Ru etch rate, Ru to SiO_2 mask etch selectivity, and etching slope with varying bias power.

sccm (Fig. 3). The source power, bias power, total gas flow rate and pressure are set to 2000 W, 300 W, 50 sccm and 30 mTorr, respectively. The $Cl_2/(O_2+Cl_2)$ gas flow ratio is set to 0.2 and the Ar flow rate varies from 0 to 10 sccm. When the Ar flow rate is 0, 5, and 10 sccm, respectively, the Ru etch rate is 280, 312, and 337 Å/min and the etching slope is 80, 81, and 81°. The Ru etch rate and the Ru to SiO_2 mask etch selectivity increase by adding Ar gas. We surmise that not only the chemical etching plays an important role, but also Ar ion bombardment affects the Ru etching process.

We demonstrate the pattering of Ru electrode with a CD of 0.15 μm. The samples are cut along the long axis of a storage node pattern. Fig. 4 shows that the Ru etching slope at the optimized etching condition is measured to be 84°.

Fig. 5 shows the TEM image of Ru etching profile using O_2/Cl_2 helicon plasma. The TEM image reveals that an additional layer is formed on top of the Ru layer. The average thickness of the additional layer is about 180 Å and 30 Å, respectively, on top of the bottom Ru layer and the sidewall Ru layer. By obtaining the diffraction pattern and employing the Fourier transformation, we reveal that most part of the additional layer corresponds to amorphous materials and some materials at point "B" and at point "C" are identified as RuO_2 (Fig. 5).

The distance between 2 adjacent crystalline plane of the material at position "B" is measured to be 3.2 Å, which corresponds to the lattice parameter of RuO_2 (110). The distance between 2 adjacent crystalline plane of the material at position "C" is measured to be 2.5 Å, which corresponds to the lattice parameter of RuO_2 (101). On the other hand, the distance between 2 adjacent crystalline plane of the material at position "A" is measured to be 2.4 Å, corresponding to the lattice parameter of Ru(100).

In order to understand the Ru etching process, we investigated the etched Ru surface using O_2 and O_2/Cl_2 plasma. We performed an XPS measurement and Table 1 shows the relative amounts of Ru, O, and Cl elements on the etched Ru surface below the depth of 100 Å. The

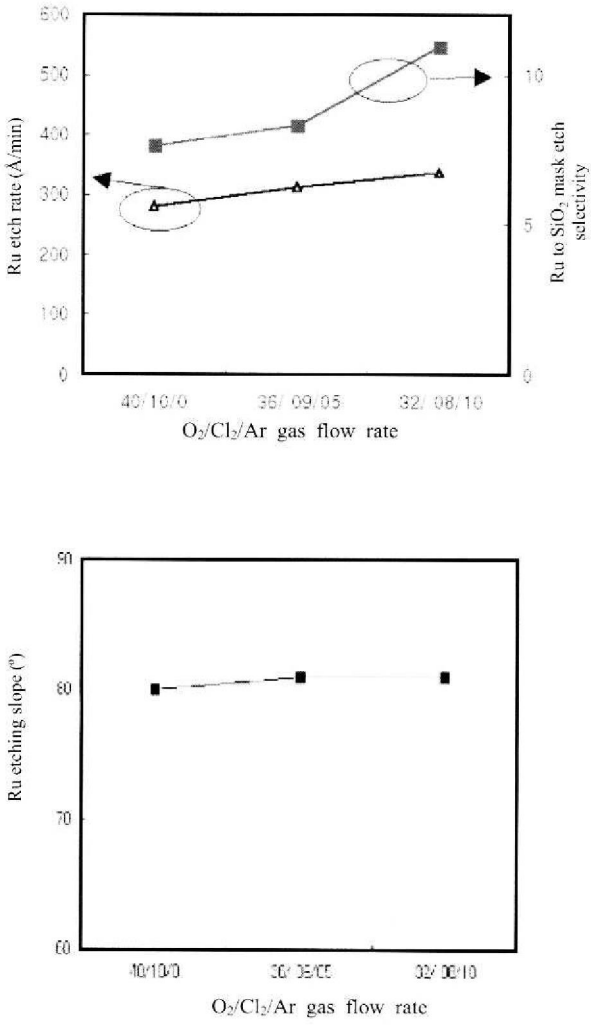

Fig. 3. Variation of Ru etch rate, Ru to SiO_2 mask etch selectivity, and etching slope with increasing Ar flow rate. The total flow rate was set to 50 sccm and the $Cl_2/(O_2+Cl_2)$ gas flow ratio was set to 0.2. The Ar flow rate was varied from 0 to 10 sccm.

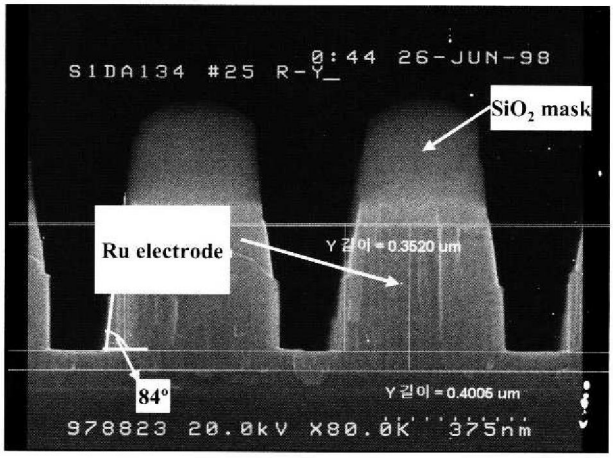

Fig. 4. SEM image of Ru etching profile.

Table 1. XPS measurement indicating the relative amounts of Ru, O, and Cl elements on the etched Ru surface below a depth of 100 Å.

Etchant	Ru	O	Cl
$O_2 / (O_2 + Cl_2) = 0.8$	54.5%	41.1%	4.3%
$O_2 / (O_2 + Cl_2) = 1.0$	38.0%	60.4%	1.6%

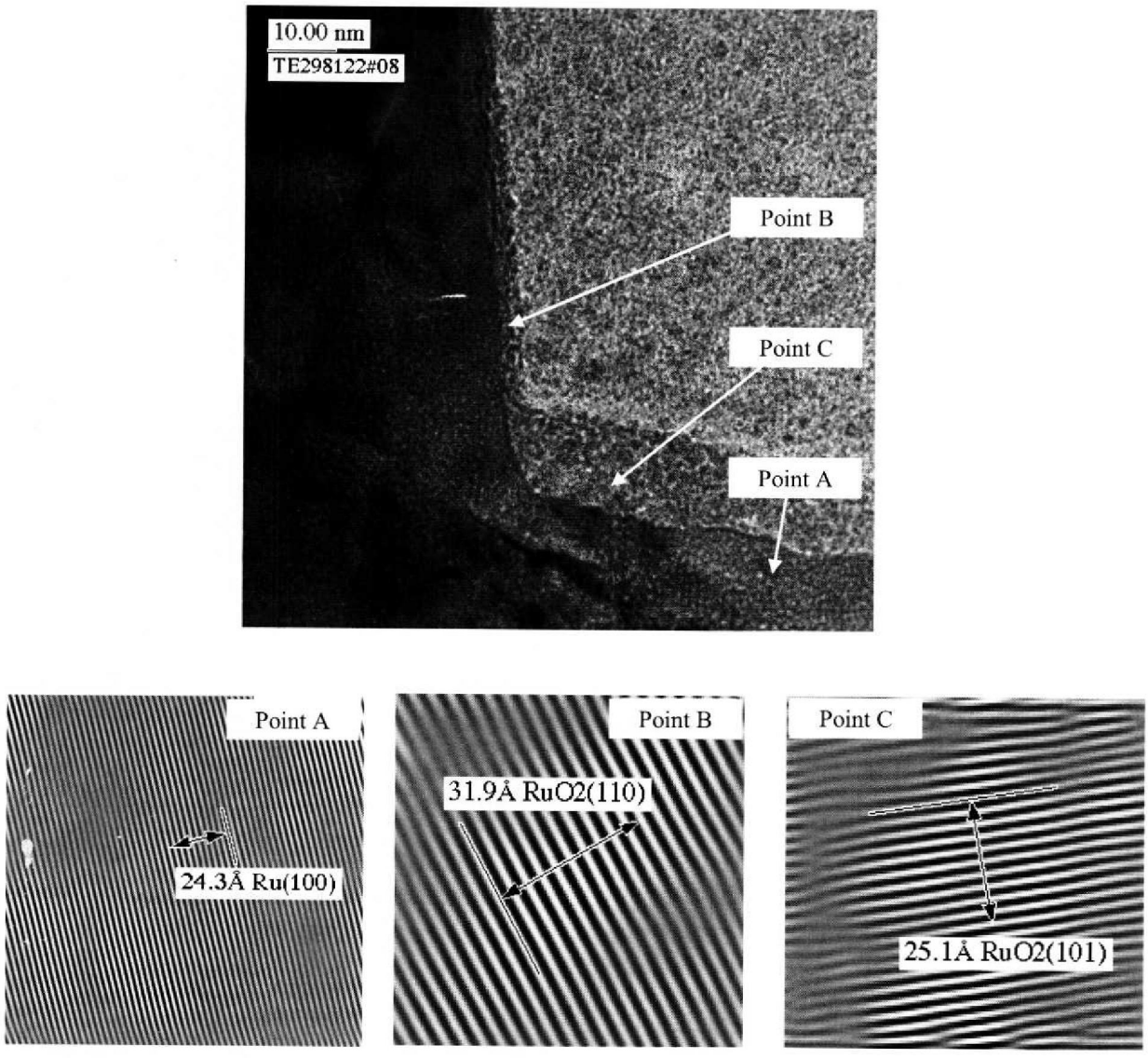

Fig. 5. TEM image of Ru etching profile.

relative amount of O element on the Ru surface etched using O_2 plasma is greater than that using O_2/Cl_2 plasma. Also, the relative amount of Cl_2 elements on the Ru surface etched using O_2 plasma is smaller than that using O_2/Cl_2 plasma.

In order to investigate the etched Ru surface, we have performed an AES analysis. The spectrum of etched Ru surface shows that the relative signal of O element compared to Ru element is greater when etched using O_2 p'asma than when etched using O_2/Cl_2 plasma (not shown here). The AES spectra agree with an XPS measurement. We surmise that Ru etching proceeds by generation of RuO_2 from Ru, and subsequent generation of volatile RuO_4 from RuO_2. Since the Ru etch rate in case of using O_2/Cl_2 plasma is greater than that in case of O_2 plasma, we surmise that high Ru etch rate occurs when the RuO_2 changes to RuO_4 efficiently. In this case, we cannot observe the RuO_x phase on the Ru surface. Further study is necessary to disclose the detailed mechanism.

4. Conclusions

Ru electrode has been etched in helicon O_2/Cl_2 discharges. The variation of Ru etch rate and Ru etching slope by varying process parameters such as $Cl_2/(O_2+Cl_2)$ gas flow ratio and bias power have been investigated. It is noteworthy that the addition of Ar gas helps to increase the Ru etch rate. TEM observation indicates that the Ru etched surface of the electrode contains a RuO_2 phase. AES and XPS analysis reveal that the relative amount of

O element on the Ru surface etched using O_2 plasma is greater than that using O_2/Cl_2 plasma.

Acknowledgment

This work was supported by Samsung Electronics. We especially thank to Dr. Chang-Jin Kang for helpful discussions. This work was also supported by INHA UNIVERSITY Research Grant through the Special Research Program in 2003 (INHA-22524).

References

1. H. W. Kim, B. S. Ju, B. Y. Nam, W. J. Yoo, C. J. Kang, T. H. Ahn, J. T. Moon, and M. Y. Lee, *J. Vac. Sci. Technol.* **A 17**, 2151 (1999).
2. T. Aoyama, S. Yamazaki, and K. Imai, *J. Electrochem. Soc.* **145**, 2961 (1998).
3. W. J. Yoo, J. H, Hahm, H. W. Kim, C. O. Jung, Y. B. Koh, and M. Y. Lee, *Jpn. J. Appl. Phys.* **35**, 2501 (1995).
4. K. Nishikama, Y. Kusumi, T. Oomori, M. Hanazaki, and K. Namba, *Jpn. J. Appl. Phys.* **32**, 6102 (1993).
5. S. Yokoyama, Y. Ito, K. Ishihara, K. Hamada, S. Ohnishi, J. Kudo, and K. Sakiyama, *Jpn. J. Appl. Phys.* **34**, 767 (1995).
6. H. W. Kim, B. S. Ju, C. J. Kang, and J. T. Moon, *Microelectronic Engineering* **65**, 185 (2003).
7. S. Saito and K. Kuramasu, *Jpn. J. Appl. Phys.* **31**, 135 (1992).
8. W. Pan and S. B. Desu, *J. Vac. Sci. Technol.* **B 12**, 3208 (1994).